Motion-blur-free LCD for high-resolution virtual reality displays

Fangwang Gou (SID Student Member)
Haiwei Chen (SID Student Member)
Ming-Chun Li
Seok-Lyul Lee (SID Fellow)
Shin-Tson Wu (SID Fellow)

Abstract — A new liquid crystal display device with fast response time, high transmittance, and low voltage for virtual reality is reported. When driven at 90 Hz with 17% duty ratio, the motion picture response time is 1.5 ms, which is comparable with cathode-ray tube, leading to indistinguishable motion blur. Moreover, this device enables high-resolution density because only one thin-film transistor per pixel is needed and it has a built-in storage capacitor.

Keywords *— vertical alignment, fringe-field switching (FFS), liquid crystal displays (LCDs), virtual reality.*

DOI # 10.1002/jsid.662

1 Introduction

The recent rapid growth of virtual reality (VR) head mounted displays has triggered an urgent need for display devices with high-resolution density and fast response time.[1,2] In a VR system, a lens is used to magnify the displayed images. Thus, if the display resolution density is inadequate, the observer will see the screen door effect. In order to achieve field of view >70^{o} and to minimize the screen door effect, VR displays require resolution density over 2000 pixels per inch. At this stage, such a high pixels per inch can be achieved by silicon-based organic light-emitting diode (OLED) microdisplays[3] and by some liquid crystal display (LCD) panels fabricated with glass-based process and special pixel design.[4] In general, OLED is a current-driven device, and it requires three to four thin-film transistors (TFTs) and two capacitors per pixel. On the other hand, LCD is voltage driven, and it only requires one switching TFT and one storage capacitor per pixel. Thus, LCD has potential to achieve higher resolution density than OLED for VR applications. However, traditional LCD modes, such as in-plane switching and fringe-field switching (FFS), suffer from slow response time, which results in motion blurs.

To speed up the response time, one approach is to use a low viscosity liquid crystal (LC) material with an ultra-thin cell gap.[5] On the device side, triode approach[6–8] achieves fast rise time and decay time, but it requires two TFTs per pixel and the transmittance is compromised.

In this paper, we report a hole-type vertical alignment (VA)-FFS mode, which is driven by the longitudinal field and the fringing field. The top substrate has a common electrode, while the bottom substrate consists of FFS structure, but with etched rounded-square hole patterns on the pixel electrode. The motion picture response time (MPRT) is 1.5 ms at 90 Hz with 17% duty ratio, leading to indistinguishable motion picture blur. Besides, our device enables a high aperture ratio because only one TFT is needed per pixel while the bottom FFS electrodes have built-in storage capacitors. As a result, high resolution is achievable. This device is attractive for the emerging VR display applications.

2 Motion picture response time

Our human eyes are always moving when we track moving objects on a display. However, in a sample-and-hold-type display such as TFT-LCDs and TFT-OLEDs, the image is hold on by TFTs in a given frame time and jumps to a different position in the next frame. As a result, the moving objects will be blurred across our retina. The perceived motion blur can be quantified by MPRT[9,10]:

$$\mathrm{MPRT} \approx \sqrt{{T_{\mathrm{LC}}}^2 + \left(0.8T_f\right)^2}. \tag{1}$$

Here, T_{LC} is the LC response time and T_f is the TFT frame time (unit: ms), which is the inverse of frame rate (f, unit: Hz):

$$f = 1000/T_f. \tag{2}$$

To minimize image blur, MPRT should be less than 1.5 ms, like the impulse-type display cathode-ray tube (CRT). By achieving this goal, we can decrease LC response time and increase frame rate. Figure 1 shows a plot of MPRT versus LC response time at different frame rates. At a given frame rate, say f = 90 Hz, we find that MPRT decreases as the LC response time decreases, but it saturates when LC response time T_{LC} ≈ 2 ms. Even if LC response time is zero

Received 02/17/18; accepted 03/26/18.
Fangwang Gou, Haiwei Chen and Shin-Tson Wu are with the College of Optics and Photonics, University of Central Florida, Orlando, FL 32816, USA; e-mail: swu@creol.ucf.edu.
Ming-Chun Li and Seok-Lyul Lee are with the AU Optronics Corp., Hsinchu Science Park, Hsinchu 30078, Taiwan.

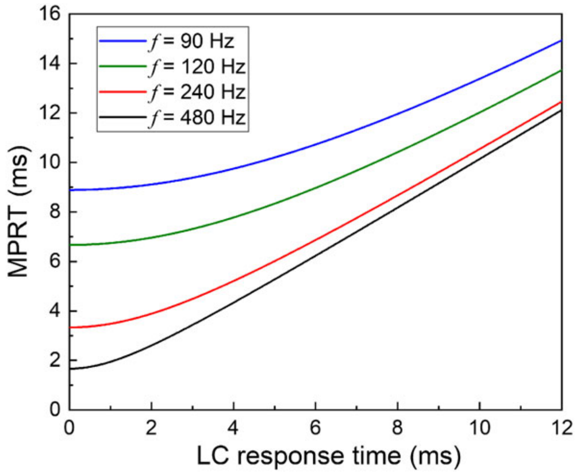

FIGURE 1 — Motion picture response time (MPRT) as a function of liquid crystal (LC) response time with different frame rates.

(T_{LC} = 0 ms), the MPRT is still as slow as 8.89 ms. This happens to OLED as well. Another trend we can see from Fig. 1 is that as frame rate increases, MPRT decreases. When f = 480 Hz and T_{LC} ≈ 2 ms, the average MPRT ≈ 2.88 ms, which is still too slow. Moreover, for a high-resolution LCD, for example, 4K2K, operating at 480 Hz frame rate would demand a very short TFT charging time (1.08 μs). This is technically challenging by itself.

A simpler way to reduce MPRT is through backlight modulation.[11] Figure 2 illustrates the scan signal timing diagram with backlight modulation. In one frame time, the backlight remains off during gate line scanning and LC transition time and then is turned on when all of the pixels have fully reached their targeted gray levels. As a result, the initial slow transition part of LC is obscured by the delayed backlight, which effectively suppresses the sample-and-hold effect. Such an operation mechanism is similar to impulse driving of CRT. The ratio of backlight turn-on time to one frame time is defined as duty ratio, and it satisfies

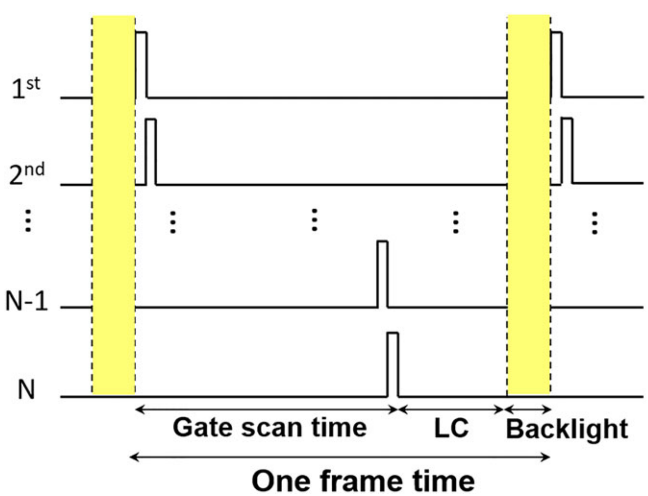

FIGURE 2 — The schematic of the data address sequence with backlight modulation.

$$T_f \times \mathrm{DR} = T_f - T_g - T_{LC}, \qquad (3)$$

where T_g is the gate scan time. Therefore, MPRT can be simplified as

$$\mathrm{MPRT} \approx 0.8 \times \left(T_f - T_g - T_{LC}\right). \qquad (4)$$

For a TFT-LCD with ~2000 gate scan lines, T_g takes 5~7 ms. In order to obtain MPRT less than 1.5 ms, we can calculate the backlight modulation duty ratio and the remaining time duration for the LC to respond. Results are plotted in Fig. 3. As the duty ratio decreases, MPRT (blue lines) decreases almost linearly, and it leaves more time in each frame for LC (black lines) to drive. The red dashed lines represent the targeted MPRT = 1.5 ms. If a display is driven at f = 90 Hz (T_f = 11.11 ms), then in order to obtain MPRT ≤ 1.5 ms, the duty ratio should be kept below 0.17. Under such condition, using Eq. (3), we obtain T_{LC} = 4.24 ms. Also from Fig. 3, if we increase frame rate to f = 120 Hz (T_f = 8.33 ms), then the required duty ratio is less than 0.22, and the remaining time duration for the LC to respond is only 1.50 ms, which is challenging for traditional LCD modes such as FFS and in-plane switching. Moreover, if the backlight turns on before all pixels finish their transitions, nonuniform motion blur will be seen in the whole display area.[12] To mitigate the LC's requirement for fast response time at higher frame rate, a low backlight duty ratio is preferred, but the major trade-off is decreased brightness. To remedy the decreased brightness, we could increase the driving current of the LED backlight or use a more efficient backlight.

3 Results and discussions

3.1 Device structure

To achieve fast response time, we proposed a hole-type VA-FFS structure as illustrated in Fig. 4(a) and 4(b). On the top substrate, it has a planar common electrode grounded at

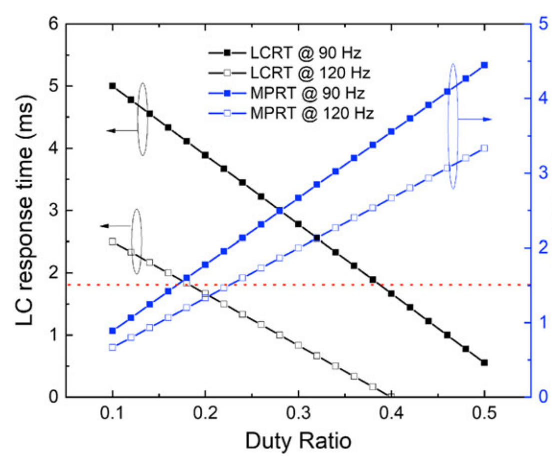

FIGURE 3 — The motion picture response time (MPRT, blue) and liquid crystal response time (LCRT, black) as a function of duty ratio with T_g = 5 ms. The red dashed lines represent MPRT = 1.5 ms.

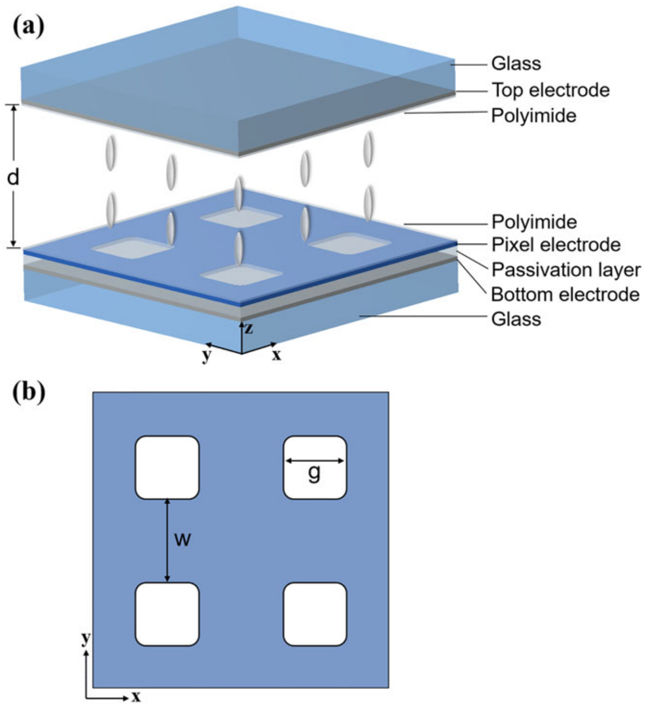

FIGURE 4 — (a) Device structure of the proposed hole-type vertical alignment–fringe-field switching cell and (b) top view of the pixel electrode.

$V = 0$. On the bottom substrate, a passivation layer is sandwiched between a pixel electrode layer and a planar common electrode layer, which is similar to the fringing field switching electrode configuration. The difference is that the pixel electrode layer is patterned with rounded-square holes, and LC with negative dielectric constant ($\Delta\varepsilon < 0$) is initially in VA. The LC material we used for simulation is ZOC-7003 (JNC, Japan) and its $\Delta\varepsilon = -4$.[13] Figure 4(b) shows the patterns and dimensions of the holes.

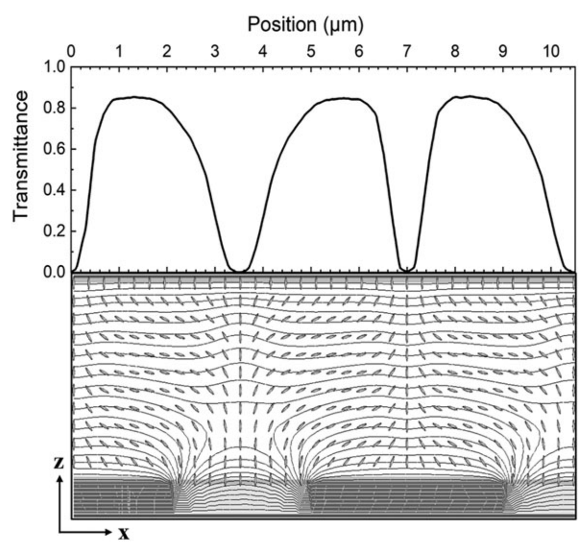

FIGURE 5 — Transmittance (upper) and cross-sectional view of simulated liquid crystal director distributions (lower) of the vertical alignment–fringe-field switching cell at 7 V_{rms}.

After optimization, we chose the electrode gap $g = 3$ μm and electrode width $w = 4$ μm for further calculations.

3.2 Voltage-dependent transmittance

To achieve high transmittance and good dark state for wide-view purpose, the LC cell is sandwiched between two circular polarizers and a set of compensation films. When the voltage is not present, all the LC directors are vertically aligned (pre-tilt angle = 0°). The light passing through the LC layer experiences no phase retardation and is blocked by the crossed circular polarizers, leading to an excellent dark state. As the voltage exceeds a threshold, the LC directors are reoriented by the vertical field outside the hole area and the fringing field surrounding the hole area. Similar to

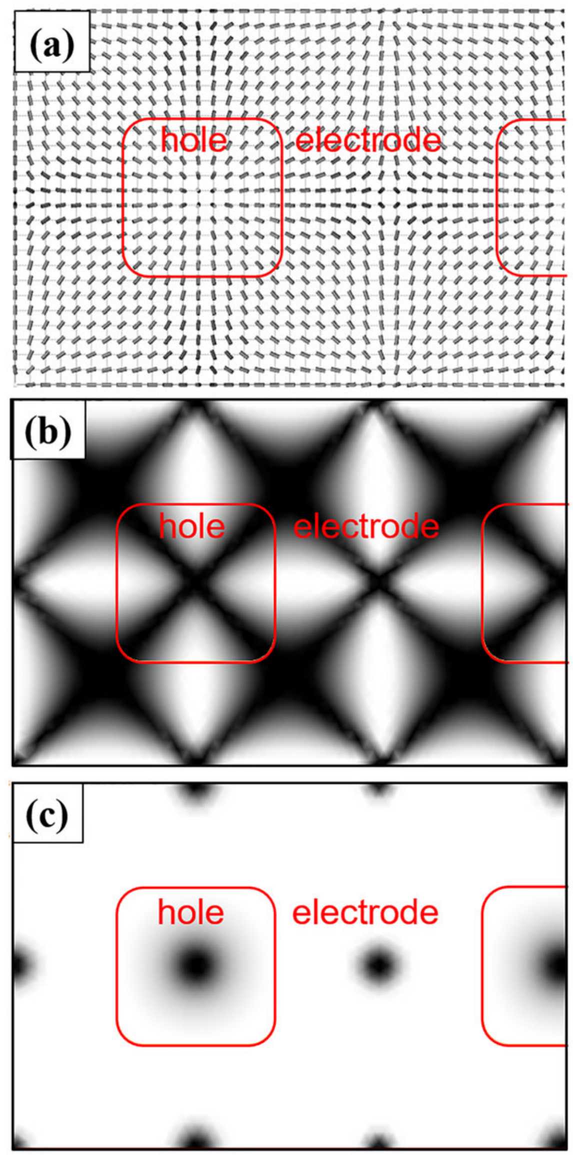

FIGURE 6 — Top view of (a) simulated liquid crystal director distributions and on-state transmittance profiles of the vertical alignment–fringe-field switching cell with crossed (b) linear polarizers and (c) circular polarizers, at $V_{on} = 7$ V_{rms}.

patterned VA mode,[14] the oblique component of the fringing field prevents LC directors from reorienting randomly even though the pre-tilt angle is 0°. Figure 5 depicts the transmittance (upper) and cross-sectional view of LC director distributions (lower) at a voltage-on state (7 V_{rms}). Because of symmetry, the LC directors at the center of the square holes and the pixel electrodes do not reorient (if the voltage is not too high), which function as standing walls to provide strong restoring force for improving decay time.[15,16] However, these vertical standing walls decrease the transmittance as shown in Fig. 5; thus, their dimensions should be optimized. Also through simulation, we found that the pixel electrode with rounded-square holes exhibits similar performance with circular or square holes,[17] indicating that our VA-FFS mode enables a relatively large fabrication tolerance.

From the top view of LC director distribution shown in Fig. 6(a), we can see that the LC directors inside the hole area are primarily affected by the symmetric fringing fields so that they are radially distributed. However, on top of pixel electrodes, the LC directors are influenced by both longitudinal and fringing fields. Because of these spatially nonuniform LC reorientations, crossed circular polarizers are preferred to achieve high transmittance. Figure 6(b) and 6(c) illustrates the top view of transmittance profiles with crossed linear polarizers and circular polarizers. For linear polarizers, the light transmitting through the first polarizer experiences no phase retardation if the LC directors distributed along the transmission axis of linear polarizer. As a result, the light will be blocked by the analyzer, leading to transmittance dead zone. In the case of crossed circular polarizers, the circularly polarized light is independent of the LC director's orientation angle; thus, a higher transmittance is achieved.

Figure 7 depicts the simulated voltage–transmittance curves of our optimized VA-FFS cell at λ = 450, 550, and 650 nm. By using circular polarizers, the peak transmittance can reach 85% at 7 V_{rms} for λ = 550 nm, which is comparable with the two-domain FFS mode using negative $\Delta\varepsilon$ LC (~85%).[18]

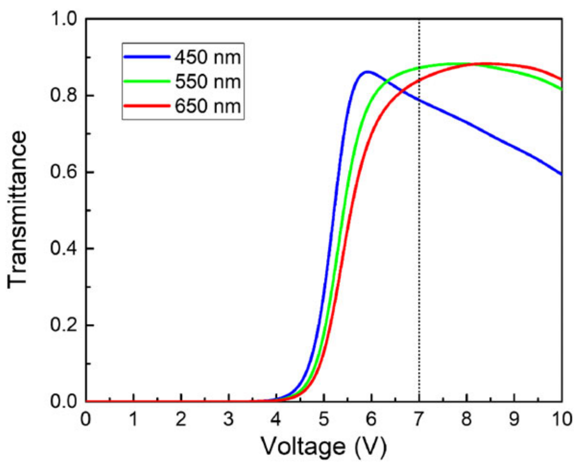

FIGURE 7 — Simulated voltage–transmittance curves of the proposed vertical alignment–fringe-field switching cell at the specified wavelengths; d = 3.5 μm, w = 4 μm, and g = 3 μm.

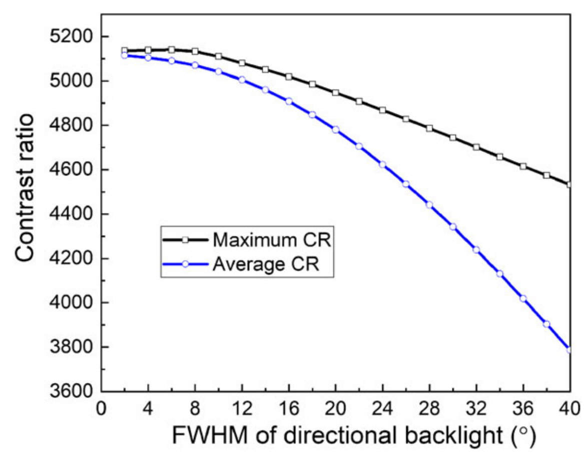

FIGURE 9 — Simulated contrast ratio (CR) of vertical alignment–fringe-field switching liquid crystal display as a function of the full width at half maximum (FWHM) of directional backlight.

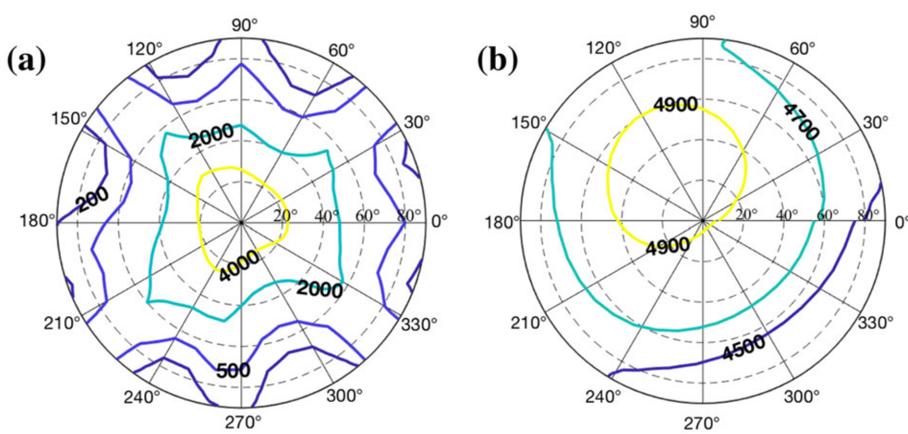

FIGURE 8 — Simulated isocontrast contours (a) with conventional backlight and (b) with directional backlight and compensation films. The full width at half maximum of the directional backlight is 20° (+10°/−10°).

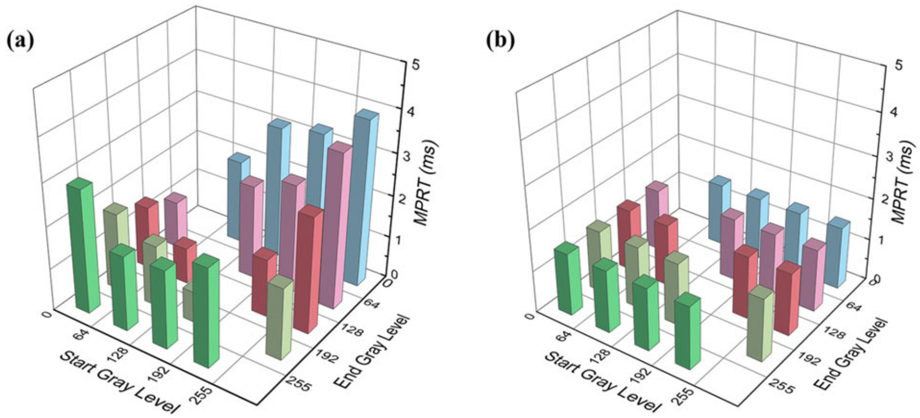

FIGURE 10 — (a) The gray-to-gray response time of the hole-type vertical alignment–fringe-field switching mode. (b) Motion picture response time (MPRT) at f = 90 Hz with duty ratio = 0.17, T_g = 5 ms.

To widen the viewing angle of an LCD, compensation films together with a directional backlight and a weak diffusive film can be employed.[19,20] In our simulation, we used the compensation scheme proposed by Ge *et al*.[21] The phase retardation from the LC layer is partially compensated by a negative C-plate, and the residual phase retardation is compensated by a biaxial film. The parameters of the negative C-plate and biaxial plate are as follows: $n_{e,C}$ = 1.5902, $n_{o,C}$ = 1.5866, $n_{x,B}$ = 1.5028, $n_{y,B}$ = 1.5000, $n_{z,B}$ = 1.5018, d_C = 21.4 μm, and d_B = 74.0 μm. For the directional backlight, it has a symmetrical round luminance cone of ±10°, which means the full width at half maximum (FWHM) of the angular luminance distribution is 20° (+10°/−10°) in all directions. Figure 8(a) and 8(b) depicts the calculated isocontrast contour of hole-type VA-FFS LCD with the conventional backlight and directional backlight, respectively. For the conventional backlight case, the maximum contrast ratio is CR ≈ 5000:1, and a contrast ratio over 200:1 covers ~80° viewing cone. By employing the directional backlight, a contrast ratio over 4500:1 is expanded to almost the entire viewing cone.

Figure 9 shows the maximum and average contrast ratios as a function of the FWHM of the directional backlight. As the FWHM decreases, the maximum contrast ratio increases linearly first and then saturates at FWHM ≈ 8° (+4°/−4°).

In addition to wide view, gamma shift is another important concern for display devices. To quantitatively evaluate the off-axis image quality, an off-axis image distortion index (D) defined in previous study[22] is used. When $D < 0.2$, the image distortion is indistinguishable by the human eye. With the directional backlight (FWHM = 20°) and diffusive film, we could achieve D = 0.064. Besides, the diffusive film could be replaced by a quantum dot array to widen the viewing angle while keeping a wide color gamut.[23]

3.3 Response time

To obtain MPRT, first we calculate the gray-to-gray response time of our VA-FFS cell. We divided the voltage–transmittance curve at λ = 550 nm into 256 gray levels and calculated the response time between different gray levels. The response time is defined as the time interval between 10% and 90% transmittance change. Results are shown in Fig. 10(a). By applying overdrive and undershoot driving scheme,[24] the average gray-to-gray response time is 2.26 ms and the slowest LC response time T_{LC} = 4.07 ms. From the aforementioned discussion in Section 2 that in order to obtain MPRT ≤ 1.5 ms at f = 90 Hz, T_{LC} should be less than 4.24 ms with duty ratio = 0.17. The final MPRT is 1.5 ms as shown in Fig. 10(b), indicating that our VA-FFS mode can achieve indistinguishable motion blur. If we further increase frame rate to 120 Hz with the same duty ratio, the MPRT will decrease to 1.13 ms, and the slowest LC response time should be less than 1.92 ms. To do so, we could employ an LC material with higher Δn and lower viscosity. However, the latter may lead to a smaller $\Delta\varepsilon$, which in turn results in slightly higher on-state voltage.

4 Conclusion

Our proposed hole-type VA-FFS mode exhibits several attractive properties: peak transmittance > 85% and low operation voltage (7 V_{rms}) by using circular polarizers and potentially high-resolution density (single TFT per pixel). By driving at 90 Hz frame rate and decreasing the duty ratio to 17%, we obtained MPRT = 1.5 ms, which is comparable with CRT. Potential application of our VA-FFS for the wearable VR displays is foreseeable.

Acknowledgment

The authors are indebted to A.U. Vista Inc. for the financial support.

References

1 O. Cakmakci and J. Rolland, "Head-worn displays: a review," *J. Disp. Technol.*, **2**, No. 3, 199–216 (2006). https://doi.org/10.1109/jdt.2006.879846.
2 S. Kawashima *et al*., "A 1058-ppi 4K ultrahigh-resolution and high aperture LCD with transparent pixels using OS/OC technology," *SID Int. Symp. Digest Tech. Papers*, **48**, No. 1, 242–245 (2017). https://doi.org/10.1002/sdtp.11679.
3 A. Ghosh *et al*., "Directly patterned 2645 PPI full color OLED microdisplay for head mounted wearables," *SID Int. Symp. Digest Tech. Papers.*, **47**, No. 1, 837–840 (2016). https://doi.org/10.1002/sdtp.10805.
4 H. S. Lee *et al*., "An ultra high density 1.96″ UHD 2250ppi display," *SID Int. Symp. Digest Tech. Papers.*, **48**, No. 1, 403–405 (2017). https://doi.org/10.1002/sdtp.11629.
5 H. Chen *et al*., "A submillisecond-response nematic liquid crystal for augmented reality displays," *Opt. Mater. Express*, **7**, No. 1, 195–201 (2017). https://doi.org/10.1364/ome.7.000195.
6 D. J. Channin, "Triode optical gate: a new liquid crystal electro-optic device," *Appl. Phys. Lett.*, **26**, No. 11, 603–605 (1975). https://doi.org/10.1063/1.88018.
7 Y. Iwata *et al*., "Novel super fast response vertical alignment-liquid crystal display with extremely wide temperature range," *J. Soc. Inf. Disp.*, **22**, No. 1, 35–42 (2014). https://doi.org/10.1002/jsid.221.
8 T. H. Choi *et al*., "Fast grey-to-grey switching of a homogeneously aligned liquid crystal device," *Liq. Cryst.*, **42**, No. 4, 492–496 (2015). https://doi.org/10.1080/02678292.2014.1000987.
9 Y. Igarashi *et al*., "Summary of moving picture response time (MPRT) and futures," *SID Int. Symp. Digest Tech. Papers*, **35**, No. 1, 1262–1265 (2004). https://doi.org/10.1889/1.1821340.
10 F. Peng *et al*., "Analytical equation for the motion picture response time of display devices," *J. Appl. Phys.*, **121**, No. 2, 023108 (2017). https://doi.org/10.1063/1.4974006.
11 H. Ito *et al*., "Evaluation of an organic light-emitting diode display for precise visual stimulation," *J. Vis.*, **13**, 6 (2013). https://doi.org/10.1167/13.7.6.
12 C.-H. Li *et al*., "The study of motion blur behavior in the strobe backlight LCD for virtual reality application," *SID Int. Symp. Digest Tech. Papers*, **48**, No. 1, 1142–1145 (2017). https://doi.org/10.1002/sdtp.11844.
13 Y. Chen *et al*., "High performance negative dielectric anisotropy liquid crystals for display applications," *Crystals*, **3**, No. 3, 483–503 (2013). https://doi.org/10.3390/cryst3030483.
14 S. H. Lee *et al*., "Electro-optic characteristics and switching principle of a nematic liquid crystal cell controlled by fringe-field switching," *Appl. Phys. Lett.*, **73**, No. 20, 2881–2883 (1998). https://doi.org/10.1063/1.122617.
15 K. H. Kim *et al*., "Domain divided vertical alignment mode with optimized fringe field effect," *Proc. Asia Display*, **98**, 383–386 (1998).
16 H. Chen *et al*., "A low voltage liquid crystal phase grating with switchable diffraction angles," *Sci. Rep.*, **7**, 39923 (2017). https://doi.org/10.1038/srep39923.
17 F. Gou *et al*., "Submillisecond-response liquid crystal for high-resolution virtual reality displays," *Opt. Express*, **25**, No. 7, 7984–7997 (2017). https://doi.org/10.1364/oe.25.007984.
18 H. Chen *et al*., "n-FFS vs. p-FFS: who wins?" *SID Int. Symp. Digest Tech. Papers*, **46**, No. 1, 735–738 (2015). https://doi.org/10.1002/sdtp.10182.
19 K. Käläntär, "A directional backlight with narrow angular luminance distribution for widening the viewing angle for an LCD with a front-surface light-scattering film," *J. Soc. Inf. Disp.*, **20**, No. 3, 133–142 (2012). https://doi.org/10.1889/jsid20.3.133.
20 Y.-J. Wang *et al*., "High directional backlight using an integrated light guide plate," *Opt. Express*, **23**, No. 2, 1567–1575 (2015). https://doi.org/10.1364/oe.23.001567.
21 Z. Ge *et al*., "Extraordinarily wide-view circular polarizers for liquid crystal displays," *Opt. Express*, **16**, No. 5, 3120–3129 (2008). https://doi.org/10.1364/oe.16.003120.
22 S. S. Kim *et al*., "New technologies for advanced LCD-TV performance," *J. Soc. Inf. Disp.*, **12**, No. 4, 353–359 (2004). https://doi.org/10.1889/1.1847732.
23 J. P. Yang *et al*., "Wide viewing angle TN LCD enhanced by printed quantum-dots film," *SID Int. Symp. Digest Tech. Papers*, **47**, No. 1, 21–24 (2016). https://doi.org/10.1002/sdtp.10588.
24 S. T. Wu, "Nematic liquid crystal modulator with response time less than 100 µs at room temperature," *Appl. Phys. Lett.*, **57**, No. 10, 986–988 (1990). https://doi.org/10.1063/1.103533.

Fangwang Gou received her BS degree from University of Electronic and Science and Technology of China in 2012 and MS degree from Peking University, China, in 2015. Currently, she is working toward the PhD degree at College of Optics and Photonics, University of Central Florida, USA. Her current research interests include liquid crystal materials and devices for display and photonic applications.

Haiwei Chen received his BS degree in Optoelectronic Information Engineering from Beihang University, Beijing, China, in 2013, and is currently working toward the PhD degree at College of Optics and Photonics, University of Central Florida, Orlando, FL, USA. His research focuses on wide color gamut, high dynamic range, and fast-response liquid crystal display devices. He received SID Distinguished Student Paper Awards in 2015 and 2016.

Ming-Chun Li received his BS degree in Electronic Engineering, Feng Chia University, Taiwan, in 2000, and MS degree from National Sun Yat-Sen University, Taiwan, in 2005. Currently, he is a manager at AU Optronics, in charge of LCD cell material and process technology development.

Seok-Lyul Lee received his BS degree in Electronic Communication Engineering, Kwangwoon University, Korea, in 1992, and MS degree from Chonbuk National University, Korea, in 2010. Currently, he is a senior manager and chief researcher at AU Optronics. He is one of the key inventors of fringe-field switching (FFS) liquid crystal display. He contributed to development and commercialization of mobile, tablet, and monitor TFT-LCD products using the FFS mode. He received SID Special Recognition Award in 2012 and SID Fellow Award in 2018.

Shin-Tson Wu is Pegasus professor at College of Optics and Photonics, University of Central Florida. He is among the first six inductees of the Florida Inventors Hall of Fame (2014) and a Charter Fellow of the National Academy of Inventors (2012). He is a Fellow of the IEEE, OSA, SID, and SPIE and an honorary professor of Nanjing University (2013) and of National Chiao Tung University (2017). He is the recipient of 2014 OSA Esther Hoffman Beller Medal, 2011 SID Slottow-Owaki Prize, 2010 OSA Joseph Fraunhofer Award, 2008 SPIE G. G. Stokes Award, and 2008 SID Jan Rajchman Prize. Presently, he is serving as SID honors and awards committee chair.